Effect of through-thickness compression on in-plane tensile strength of glass/epoxy composites: experimental study

Effect of through-thickness compression on in-plane tensile strength of glass/epoxy composites: Experimental study

Deng'an Cai [a, b], Guangming Zhou [a, *], Vadim V. Silberschmidt [b]

[a] *State Key Laboratory of Mechanics and Control of Mechanical Structures, Nanjing University of Aeronautics and Astronautics, PR China*
[b] *Wolfson School of Mechanical and Manufacturing Engineering, Loughborough University, UK*

ABSTRACT

The effect of through-thickness compression on in-plane tensile strength of glass/epoxy composites with random microstructure was investigated experimentally. The studied composite laminates were manufactured with a self-regulating Resin Transfer Moulding device. Their mechanical behaviour was assessed in pure in-plane tensile and through-thickness compressive tests, followed by biaxial tests combining both loading modes; indenters with a radius ranging from 5 to 25 mm were used to impose a compressive mode. The obtained results demonstrate a nonlinear decreasing trend for the in-plane tensile strength under the growing through-thickness compressive stress. All the failed specimens showed catastrophic brittle failure with a specific fracture orientation that mainly exhibited a tensile mode of fibre fracture for smaller radii of indenters and a combination of matrix crack, fibre fracture and typical shear failure for larger radii.

1. Introduction

The main reasons for increasing popularity of fibre-reinforced polymer (FRP) composites in weight-critical applications are their high specific stiffness and strength. Among examples of engineering applications where FRP composites have become indispensable are sporting goods, aerospace, automotive and naval structures and components [1,2]. With the increasing use of composite materials, biaxial or multiaxial stress states can often be found in structural elements. Therefore, the need to deal with a response of composite structures to complex loading conditions becomes more important [3,4].

Problems of multiaxial stress in composites have attracted attention of various researchers, including also those involved in Worldwide Failure Exercises (WWFE-I, II and III) [5e7]. However, there is still a paucity of reliable experimental data for biaxial or multiaxial loading cases, due to high cost and complexity of multiaxial testing. In recent years, a number of works have investigated planar biaxial tension/compression behaviour of FRP composites. A study by Smits et al. [8] suggested a new cruciform type of a specimen for obtaining reliable biaxial failure data for

composites based on finite-element simulations of such specimens combined with respective experiments. Subsequently, shape optimization of these specimens for biaxial testing was investigated in some works [9,10]. A generic optimization process based on the finite-element approach was developed to provide geometry modifications that could fulfil predefined requirements for a successful biaxial test. The experimental results obtained with a Digital Image Correlation (DIC) method were in a good agreement with numerical ones. The influence of the geometrical design and differences between 2D and 3D finite-element models of a biaxially loaded cruciform specimen are also significant [11,12]. Additionally, many scientists also focused on failure criteria and envelopes for FRP composites under biaxial loadings conditions [13e18].

However, the research of multiaxial loading cases involving a combination of through-thickness compression and in-plane tension is still insufficient in spite of a considerable number of works about planar biaxial loading. Chen et al. [19] studied tensile properties of a carbon-fibre 2D woven reinforced polymer-matrix composite in a through-thickness direction and found that the specimens remained linearly elastic before breakage and the tensile strength was influenced by the loading rate significantly. A novel testing method to measure through-thickness properties of thick composite laminates was also presented [20]. In that work, specimens and testing methods were developed to assess through-thickness behaviour of thick composites, and the parallel waist
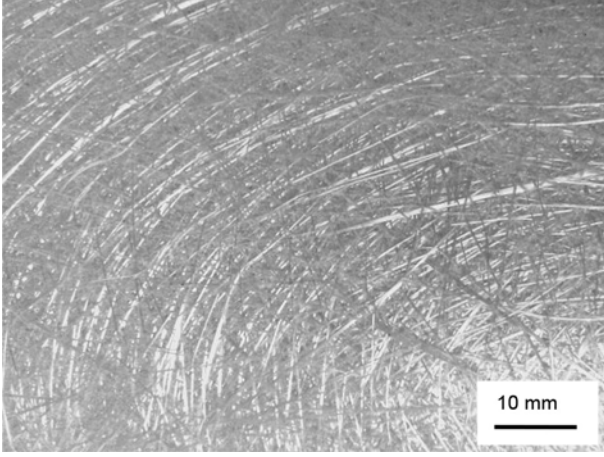
Fig. 1. Mat with random distribution of glass fibres.

block specimens were found to be sensitive to misalignment and initial machining-induced damage. Some researchers such as Deteresa et al. [21,22] found that through-thickness compression could improve the interlaminar shear strength of laminates. Gan et al. [23] showed that interaction between compressive through-thickness stress and out-of-plane shear enhanced the magnitude of shear stress of an onset of delamination in composite materials and components. Similarly, tensile strength of carbon/epoxy laminates in the fibre direction under the influence of through-thickness compressive stresses was experimentally investigated [24], and the results demonstrated that there was a linear decrease in this strength with the growing mean through-thickness stress.

In this paper, the effect of through-thickness compressive stresses on in-plane tensile strengths of glass/epoxy composite laminates was investigated experimentally. Multiple experimental load cases with a broad range of through-thickness compression and in-plane tension are presented.

2. Material and methods

2.1. Materials and manufacturing process

The material under consideration was a glass fibre-reinforced epoxy system. Several identical panels consisting of ten similar plies were fabricated. The reinforcement used in this study was a mat of E-glass fibres (diameter 12 mm and length 8℮12 cm), randomly oriented in its plane, with the areal density of 214 g/m^2 (Fig. 1), with the matrix material being epoxy resin WSR618. Benzene dimethylamine was used as a resin-curing agent, and butyl phthalate as viscous additive. The studied composite laminates were manufactured with a self-regulating Resin Transfer Moulding (RTM) device, employing pressed infiltration and a spontaneous curing process (Fig. 2). This device comprised a braced steel frame, a screw rod, a fixed plate, a nut, a load sensor, a pressure indenter, a piston, a resin tank and a flat workbench. To manufacture the composites, first, the mats with random glass fibres were placed in the mould with a sealed cavity, and then the resin, curing agent and viscous additive were added to the resin tank after being mixed properly. Then, the resin tank and the injection port of the mould were connected hermetically. The piston was moved downward to impel the resin compound to flow into the cavity to impregnate the fibre mats when the nut was turned clockwise. Injection pressure was measured and displayed with the load sensor, which controlled the load not to exceed 1.5 kN and terminated the process when the excess resin flowed out from an export hole of the mould. Finally, the preform was cured at room temperature for 12 h and then at 60 ℃ for 3 h, completing preparation of the sample material.

2.2. Specimens and rig setup

The manufactured panels were cut into pieces of appropriate size for experiments. The actual mean thickness of the laminates was 4.68 mm. In order to avoid damage in mechanical grips, end tabs (50 mm long, made of cross-plied glass/epoxy) were glued to both ends of the specimens, leaving a 200 mm-long gauge section to adapt to a measuring space of the test equipment. Specimens of 15 mm width (Fig. 3) were cut from the panels using a water-cooled diamond wheel cutter. For accurate stress calculation, the width and thickness of every specimen were measured.

The tests were carried out on a SDS100 electro-hydraulic servo biaxial testing machine, at Nanjing University of Aeronautics and Astronautics (NUAA, China) which had a capacity of ±100 kN in each of two orthogonal directions. Four independent servo-hydraulic cylinders could implement biaxial static/fatigue tension or compression loads with any biaxial ratios. The test rig had three control modes ℮ displacement, load and deformation, and these modes could be switched between each other smoothly at

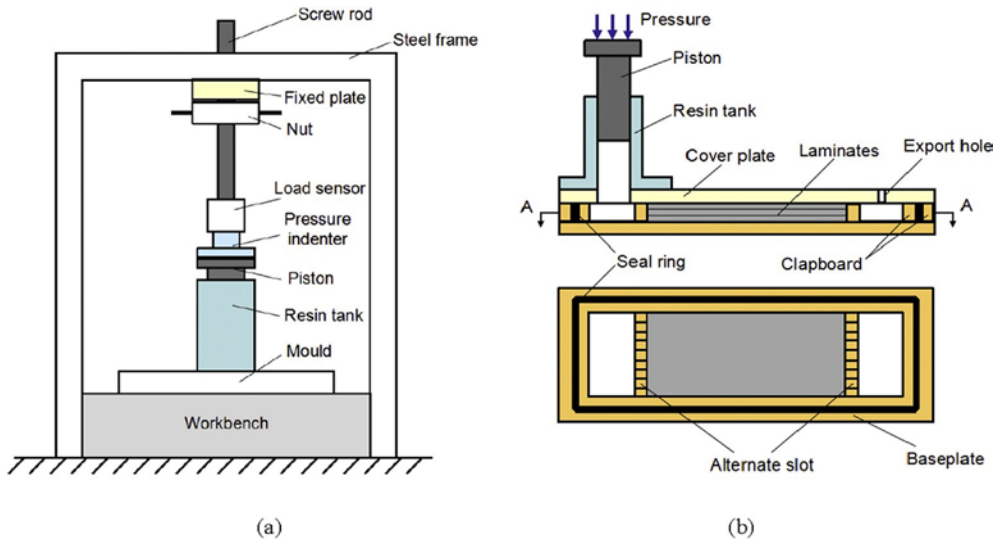(a)   (b)

Fig. 2. Self-regulating RTM device: (a) general schematic; (b) RTM mould with sealed cavity.
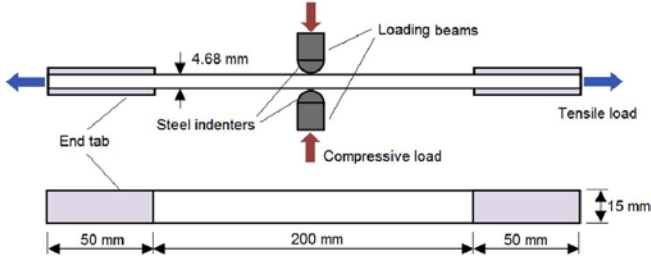
Fig. 3. Dimensions and loading of specimen.

hydraulic pressure. In tests, a pair of actuators was used for in-plane tension while another pair was employed in the perpendicular direction for through-thickness compression employing an assembly of loading beams with cylindrical steel indenters (Fig. 3). Both the displacement and load could be monitored and controlled independently for all four actuators. The localised through-thickness compressive loading was applied via a pair of heat-treated steel (30 Cr, A20302) indenters with different radii of curvature. Five radii (R ¼ 5 mm, 10 mm, 15 mm, 20 mm and 25 mm) were used to develop different levels of through-thickness compression.

2.3. Test details

Before the main biaxial loading tests, in-plane tension and through-thickness compression tests were completed separately. For the in-plane tension test, one of longitudinal actuators was locked in position and another was employed in a displacement-control mode with the in-plane tensile load applied at a rate of 0.01 mm/s (Fig. 4a). For the through-thickness compression test, the length of a specimen was half of the original (Fig. 4b), shown in Fig. 3. The specimen was just clamped by one of longitudinal actuators to eliminate the effect of redundant end restraint, and two transversal actuators were brought in until the steel indenters just touched the specimen. Then the specimens were loaded under displacement control at the rate of 0.01 mm/s with indenters of five different radii.

For the biaxial loading test (Fig. 4c), after a specimen was clamped in position by two longitudinal actuators, the two transverse steel indenters were moved to touch the specimen and were then set in the displacement-control mode with the same rate of pure through-thickness compression. The two indenters loaded the specimen synchronously to keep the symmetrical loading conditions and to avoid unwanted bending. After the compressive load reached a prescribed quantity (i.e. 5 kN, 10 kN, 15 kN, 20 kN and 25 kN) and stabilised, the control mode of transverse indenters were switched to load control to hold the compressive load constant. Then, both longitudinal actuators loaded the specimen simultaneously under displacement control, each at the same rate (to realise pure in-plane tension) to ensure the symmetry of the loading condition and also to minimise the influence of friction between the indenters and the specimen [24]. All the specimens were loaded until their catastrophic failure. The failure surfaces of the specimens were observed with a digital camera and scanning electron microscopy (SEM, JEOL JSM-6360).

3. Results and discussion

3.1. Experimental results

The test results of three types of tests ℮ in-plane tension, through-thickness compression and in-plane tension under through-thickness compression ℮ are summarized in Table 1. Three or four specimens were used for each test, and each result in the
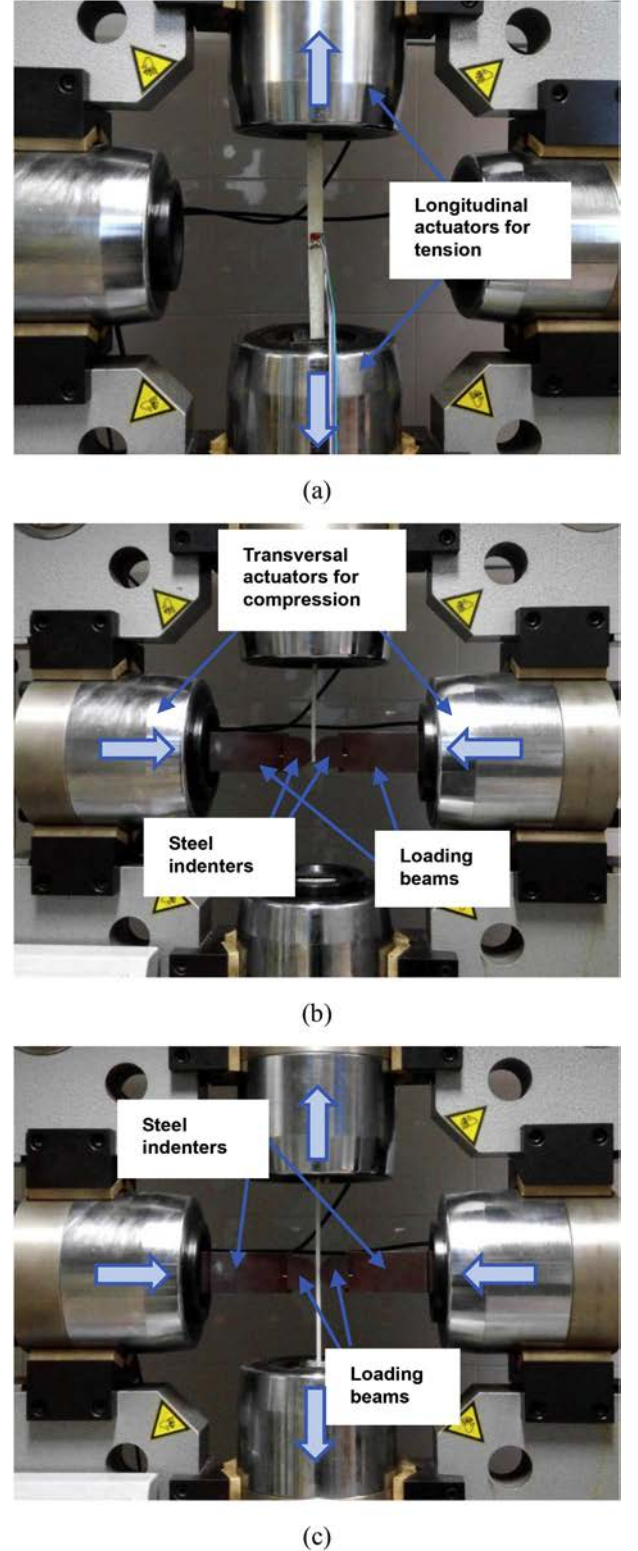

Fig. 4. Test configuration and loading fixture: (a) in-plane tension; (b) through-thickness compression; (c) in-plane tension under through-thickness compression.

table is a mean value. For the second type of tests, a significant increase in the ultimate through-thickness compressive load with the growing radius of indenters was observed. The contact width, shown in Fig. 5, i.e., the width of the contact area between the indenter and the specimen, also increased with the radius of indenters. The contact area was identified by marking its edges with

Table 1
Experimental results for random glass/epoxy composites subjected to three types of loading.

Type	Radius of indenter, R (mm)	Average actual specimen width, w (mm)	Contact width, a (mm)	Through-thickness compressive load, F_c (kN)	Tensile failure load, F_t (kN) (C.V.)
1		15.32			11.48
2	5	15.61	4.82	12.30	
	10	15.53	5.41	14.29	
	15	15.56	6.12	18.12	
	20	15.45	7.20	24.28	
	25	15.62	8.53	31.64	
3	5	14.56	4.89	5	4.68 (7.6%)
		14.66	5.01	10	1.87 (25.2%)
	10	14.64	5.52	5	6.72 (6.8%)
		14.60	6.19	10	3.02 (22.6%)
	15	14.83	5.92	5	8.52 (5.1%)
		14.84	8.41	10	3.86 (12.89%)
		14.32	10.23	15	2.17 (18.5%)
	20	14.35	6.61	5	9.11 (5.6%)
		14.82	9.57	10	4.84 (10.3%)
		14.31	10.79	15	2.81 (20.1%)
	25	14.86	7.11	5	9.87 (4.7%)
		14.37	10.49	10	5.53 (8.3%)
		14.78	11.30	15	3.27 (11.5%)

an ink wire during the test. Two additional specimens for each load case were used to measure the contact width at 67% of the ultimate through-thickness compressive load in the second type of tests (pure compression) and at 67% of the tensile failure load in the third type of tests (biaxial loading), because the contact width cannot be measured correctly when the specimen fractures. It was supposed that there would be a negligible change in the contact area after marking until ultimate failure.

The load cases of in-plane tension under through-thickness compressive load of 15 kN with the indenters with R ¼ 5 mm and R ¼ 10 mm were cancelled due to lower through-thickness compressive failure loads (i.e., 12.30 kN and 14.29 kN). For the load cases with the same indenter, in-plane tensile failure load reduced markedly under application of through-thickness compressive loads. For the load cases with the same through-thickness compressive load, the in-plane tensile failure load increased gradually with the radius of indenter. It is worth noting that 5 kN compression with the indenter with R ¼ 25 mm resulted in the maximum tensile failure load in all the load cases ⊖ 9.87 kN, which was still lower than the pure in-plane tensile failure load of 11.48 kN.

To present the failure envelope for the studied biaxial load cases with different indenter radii, the mean stress corresponding to the failure loads was adopted. The in-plane tensile stresses were calculated from the in-plane tensile failure loads by dividing the loads by the respective cross-sectional areas of the specimens, while the through-thickness compressive stresses were normalised by dividing the through-thickness compressive loads by the measured contact areas. Although the peak through-thickness compressive stresses under the indenters are higher than the calculated mean values and better characterise the compressive stresses in the loaded specimens, the latter can be directly acquired from the test. So, the mean through-thickness compressive stresses were used in this work. The results obtained in the experiments are shown in Fig. 6.

Mean compressive stresses obtained from the experimental data are between 40 MPa and 140 MPa for three compressive loads of 5 kN, 10 kN and 15 kN and five different radii of indenters. The mean through-thickness compressive strength of the laminate is the average stress obtained from five pure through-thickness compressive failure loads in Table 1. A nonlinear decreasing trend of the in-plane tensile strength is observed for the through-thickness compressive stress from 47.32 MPa to 136.15 MPa. This trend is consistent with a quadratic polynomial (Fig. 6), with the squared correlation coefficient of 0.947. The decline stabilizes at the strength level of some 30 MPa. A serious concern is that the
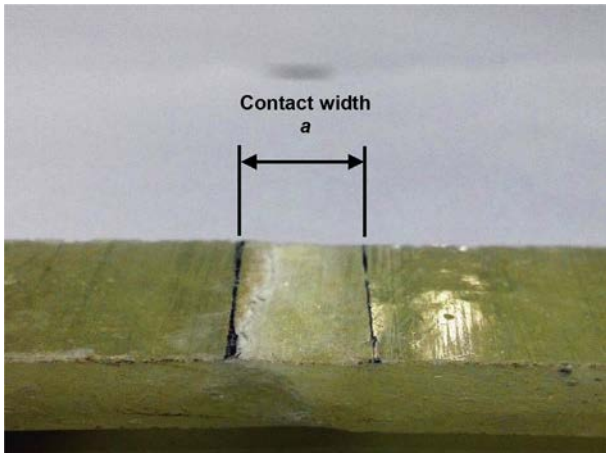

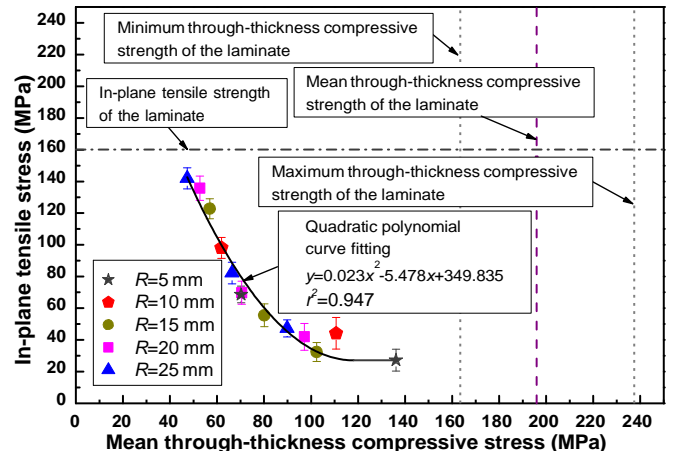Fig. 5. Contact width between indenter and specimen under through-thickness compression.

Fig. 6. Failure envelope of random glass/epoxy composites under biaxial through-thickness compression and in-plane tension.
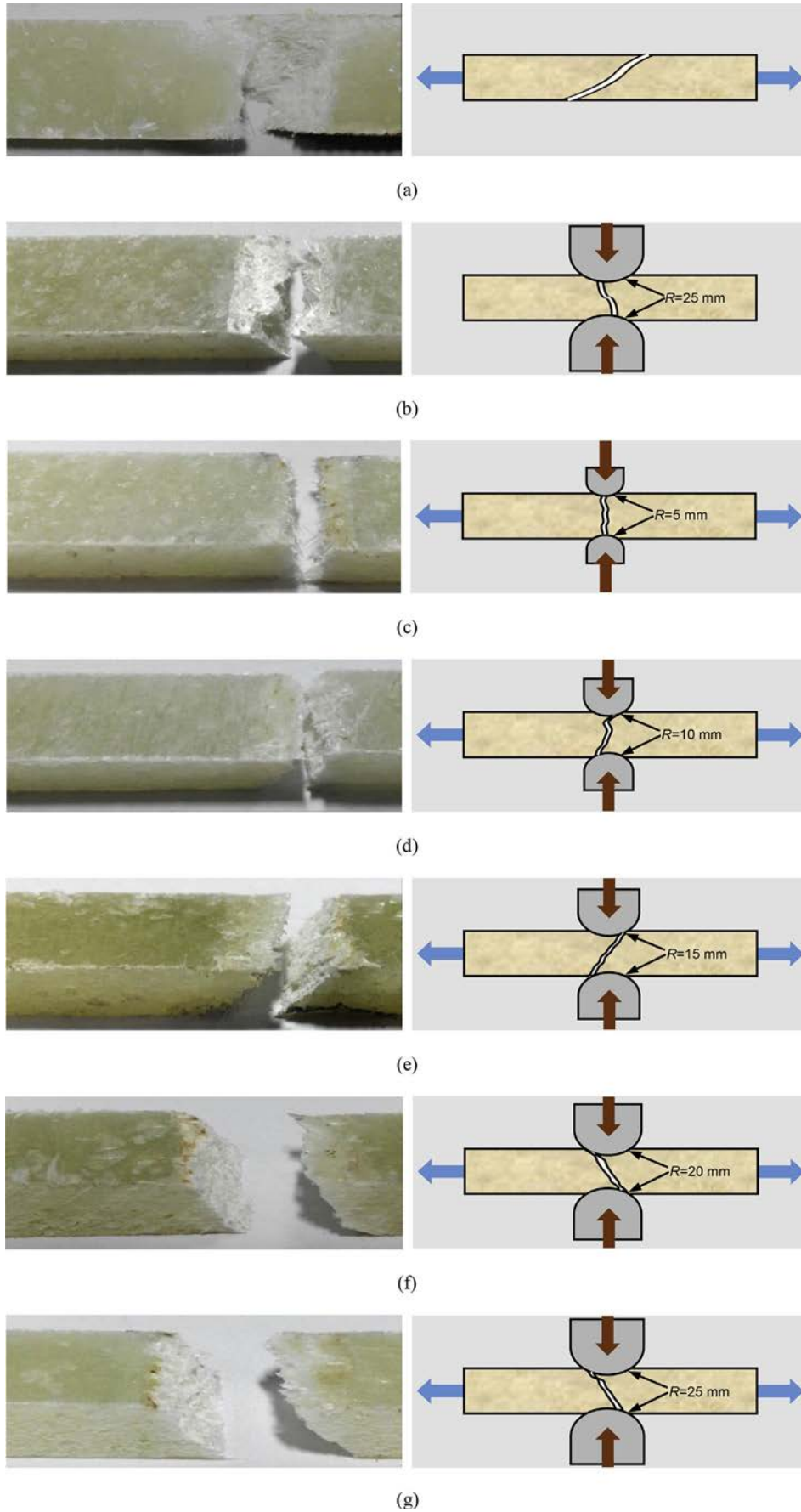
Fig. 7. Failure surfaces of specimens of random glass/epoxy composite and schematics of loading cases: (a) pure in-plane tension; (b) pure through-thickness compression (R ¼ 25 mm); (c)∈(g) in-plane tension under different through-thickness compression loads with indenters of different radii of curvature: (c) R ¼ 5 mm under 5 kN; (d) R ¼ 10 mm under 10 kN; (e) R ¼ 15 mm under 5 kN; (f) R ¼ 20 mm under 10 kN; (g) R ¼ 25 mm under 15 kN.

material shows a notable phenomenon of weakening in the biaxial load cases. For instance, the maximum in-plane tensile strength of 141.92 MPa was obtained for through-thickness compressive stress of 47.32 MPa (corresponding to 5 kN compressive load) with indenters R ¼ 25 mm, which is 88.6% of the pure in-plane tensile strength (i.e., 160.12 MPa). And the minimum tensile strength of 27.26 MPa was obtained for compressive stress of 136.15 MPa (corresponding to 10 kN compressive load) with indenters R ¼ 5 mm, which is 17.0% of the pure in-plane tensile strength.

3.2. Failure surface and microstructure

Macroscopically, all the fracture surfaces including those under pure in-plane tension and pure through-thickness compression show brittle failure with a specific fracture orientation in different load cases. The morphologies of the fracture surfaces show that the failure occurred catastrophically. The fracture surfaces of partially failed specimens are shown in Fig. 7.

For the pure in-plane tension, the failed unidirectional laminates often presented a broom-like failure with significant fibre pull-out due to fibre-bundle fracture [24,25]. However, the glass/epoxy composite laminates with random distribution of fibres show a different fracture performance under uniaxial tension, which is seen in Fig. 7a. There is a small failure area in the specimen and no signs of broom-like or splitting fibre-bundle failure. Fig. 7b shows the fracture surface of a specimen under pure through-thickness compression with the indenter with R ¼ 25 mm. The specimen demonstrates a flat fracture surface at an angle of about 80° with the longitudinal direction, excluding the creasing damage produced by the indenters on the specimen's surface. Fig. 7c exhibits a failure surface of the specimen subjected to through-thickness compression of 5 kN with indenters with R ¼ 5 mm, whereas Fig. 7d corresponds to the case with 10 kN and R ¼ 10 mm. In both cases, the failure surfaces are mainly flat and nearly
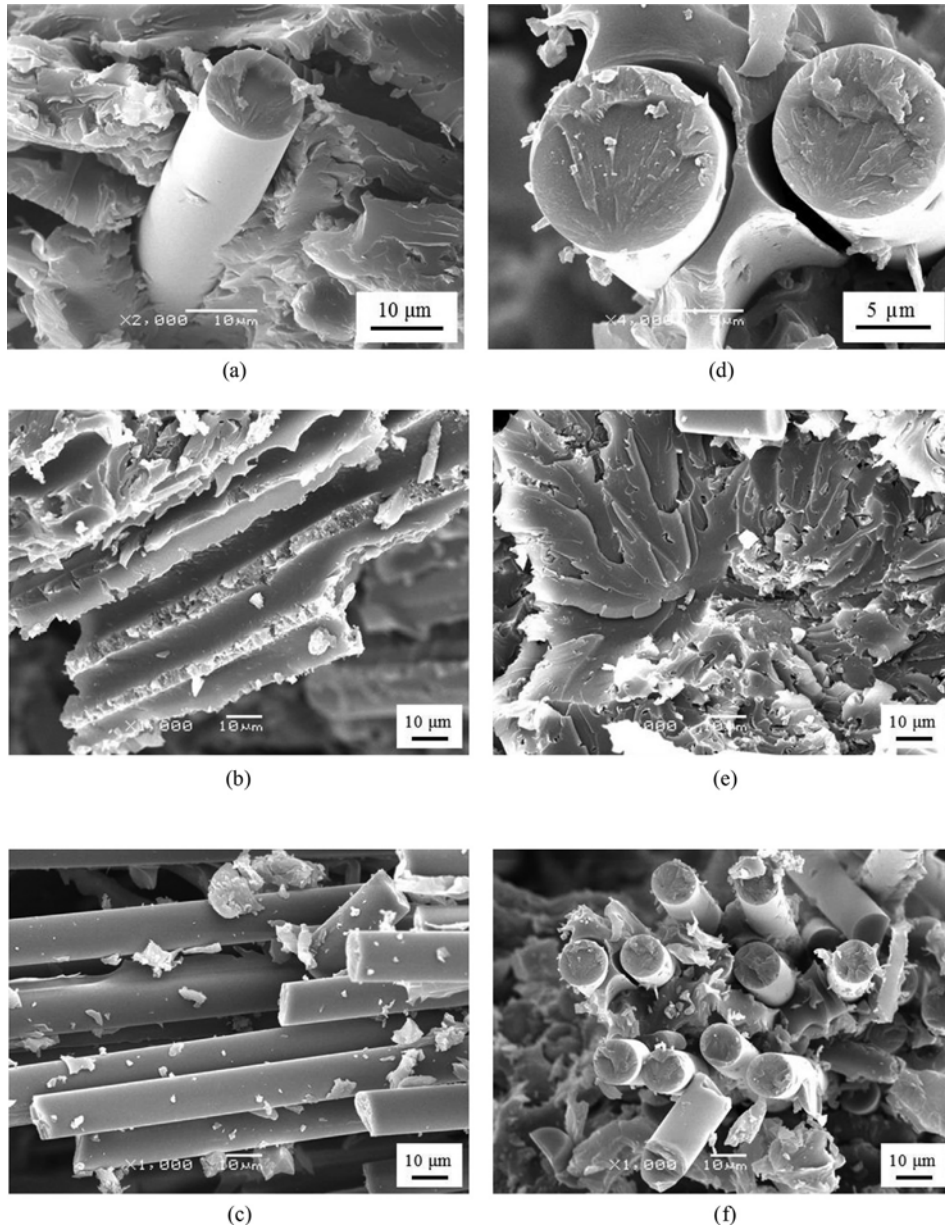

Fig. 8. SEM images of fracture surfaces of random glass/epoxy composites under biaxial loadings with different indenters: (a)∈(c) 5 kN through-thickness compression with indenters with radius of curvature R ¼ 5 mm; (d)∈(f) 15 kN through-thickness compression with indenters with radius of curvature R ¼ 25 mm: (a) and (d) ∈ fibre/matrix interface; (b) and (e) ∈ matrix crack; (c) and (f) ∈ fibre pull-out and fracture.

perpendicular to the longitudinal direction, with slight surface indentation. Similarly, Fig. 7e, f, and g clearly reveal that the failure surfaces under through-thickness compression with indenters with R ¼ 15 mm, R ¼ 20 mm and R ¼ 25 mm, respectively, exhibit a clean wedge-like failure surface at an angle of about 45⁰ with the longitudinal direction, which is a failure mode due to matrix cracks and fibre fractures accompanied by a typical shear failure mode. Although the compression-load cases are different, the failure surfaces under the indenters with larger radii of curvature show a similar fracture mode, which obviously differs from the failure mode under the indenters with R ¼ 5 mm and R ¼ 10 mm. It means that different indenters with various magnitudes of the indenter's radius led to different failure modes, but it is not possible to define exactly the critical point of the failure-mode transition depending on these limited tests.

It is known that the mechanical properties of composites are closely related to their structure and the macroscopic failure modes are even more dependent on microscopic damage mechanisms. SEM images of the fracture surfaces of the specimens subjected to biaxial through-thickness compression and in-plane tension (Fig. 8) provide some useful insights into them. Fig. 8a and d shows a clear gap between the fibre and matrix, indicating weak strength of the fibre/matrix interface. More pronounced interfacial debonding is observed for 15 kN through-thickness compression with indenters with R ¼ 25 mm (Fig. 8d) than that for 5 kN and R ¼ 5 mm (Fig. 8a). As seen from Fig. 8b, a matrix crack and the trace left by fibre pull-out can be observed. A similar matrix crack is also noticeable in Fig. 8e, which shows a petal-like trace after the fibre pull-out. As shown in Fig. 8c and f, a clear tensile fibre-failure mode with fibre pull-out is prominent. Note that the fibre surface and the matrix debris are compatible, and there are more matrix debris and broken fibres in Fig. 8f due to the effect of higher through-thickness compressive stress.

4. Conclusions

The experimental study presented in this paper is focused on the effect of through-thickness compression on the in-plane tensile strength of glass/epoxy composite laminates with random distribution of fibres exposed to biaxial loading conditions; a self-regulating RTM device was proposed to manufacture such laminates. A number of in-plane tension, through-thickness compression and biaxial loading experiments were carried out on specimens of these laminates to obtain the respective levels of strength in pure uniaxial and biaxial loading modes. It was found that through-thickness compressive stress can significantly reduce the in-plane tensile strength. The influence of three through-thickness compressive loads on the in-plane tensile strength was investigated using indenters with five different radii. A nonlinear decreasing trend described by a quadratic polynomial for the in-plane tensile strength was observed based on the data of the biaxial test results. All the failed specimens showed primarily brittle failure with a specific fracture orientation, mainly exhibiting a fibre tensile mode of failure for lower radii of indenters and a combination of matrix crack, fibre fracture and typical shear failure for higher ones.

Funding

References

[1] T.P. Sathishkumar, S. Satheeshkumar, J. Naveen, Glass fiber-reinforced polymer composites ℮ a review, J. Reinf. Plast. Compos. 33 (13) (2014) 1258℮1275.
[2] C. Soutis, Fibre reinforced composites in aircraft construction, Prog. Aerosp. Sci. 41 (2) (2005) 143℮151.
[3] R. Olsson, A survey of test methods for multiaxial and out-of-plane strength of composite laminates, Compos Sci. Technol. 71 (6) (2011) 773℮783.
[4] M. Quaresimin, L. Susmel, Multiaxial fatigue behaviour of composite laminates, Key Eng. Mater. 221 (2001) 71℮80.
[5] M.J. Hinton, A.S. Kaddour, P.D. Soden, Failure Criteria in Fibre Reinforced Polymer Composites: the World-wide Failure Exercise, Elsevier, 2004.
[6] M.J. Hinton, A.S. Kaddour, The background to the second world-wide failure exercise, J. Compos. Mater. 46 (19℮20) (2012) 2283℮2294.
[7] A.S. Kaddour, M.J. Hinton, P.A. Smith, S. Li, The background to the third world-wide failure exercise, J. Compos. Mater. 47 (20℮21) (2013) 2417℮2426.
[8] A. Smits, D. Van Hemelrijck, T.P. Philippidis, A. Cardon, Design of a cruciform specimen for biaxial testing of fibre reinforced composite laminates, Compos Sci. Technol. 66 (7) (2006) 964℮975.
[9] A. Makris, T. Vandenbergh, C. Ramault, D. Van Hemelrijck, E. Lamkanfi, W. Van Paepegem, Shape optimisation of a biaxially loaded cruciform specimen, Polym. Test. 29 (2) (2010) 216℮223.
[10] E. Lamkanfi, W. Van Paepegem, J. Degrieck, Shape optimization of a cruciform geometry for biaxial testing of polymers, Polym. Test. 41 (2015) 7℮16.
[11] E. Lamkanfi, W. Van Paepegem, J. Degrieck, C. Ramault, A. Makris, D. Van Hemelrijck, Strain distribution in cruciform specimens subjected to biaxial loading conditions, Part 1: two-dimensional versus three-dimensional finite element model, Polym. Test. 29 (1) (2010) 7℮13.
[12] E. Lamkanfi, W. Van Paepegem, J. Degrieck, C. Ramault, A. Makris, D. Van Hemelrijck, Strain distribution in cruciform specimens subjected to biaxial loading conditions, Part 2: influence of geometrical discontinuities, Polym. Test. 29 (1) (2010) 132℮138.
[13] W.P. Lin, H.T. Hu, Parametric study on the failure of fiber-reinforced composite laminates under biaxial tensile load, J. Compos. Mater. 36 (12) (2002) 1481℮1503.
[14] L. Mailly, S.S. Wang, Recent development of planar cruciform experiment on biaxial tensile deformation and failure of unidirectional glass/epoxy composite, J. Compos. Mater. 42 (13) (2008) 1359℮1379.
[15] A.E. Antoniou, D. Van Hemelrijck, T.P. Philippidis, Failure prediction for a glass/epoxy cruciform specimen under static biaxial loading, Compos. Sci. Technol. 70 (8) (2010) 1232℮1241.
[16] S. Moreno, J.J. López Cela, Failure envelope under biaxial tensile loading for chopped glass-reinforced polyester composites, Compos. Sci. Technol. 72 (1) (2011) 91℮96.
[17] S. Moreno, J.L. Martínez Vicente, J.J. López Cela, Failure strain and stress fields of a chopped glass-reinforced polyester under biaxial loading, Compos. Struct. 103 (2013) 27℮33.
[18] S.B. Sapozhnikov, S.I. Cheremnykh, The strength of fibre reinforced polymer under a complex loading, J. Compos. Mater. 47 (20℮21) (2013) 2525℮2552.
[19] D. Chen, F. Lu, B. Jiang, Tensile properties of a carbon fibre 2D woven reinforced polymer matrix composite in through-thickness direction, J. Compos. Mater. 46 (26) (2012) 3297℮3309.
[20] Y.T. Li, X.T. Zheng, G. Luo, A novel testing method for measuring through-thickness properties of thick composite laminates, Key Eng. Mater. 525℮526 (2013) 381℮384.
[21] S.J. DeTeresa, D.C. Freeman, S.E. Groves, The effects of through-thickness compression on the interlaminar shear response of laminated fiber composites, J. Compos. Mater. 38 (8) (2004) 681℮697.
[22] R.M. Christensen, S.J. DeTeresa, Delamination failure investigation for out-of-plane loading in laminates, J. Compos. Mater. 38 (24) (2004) 2231℮2238.
[23] K.W. Gan, S.R. Hallett, M.R. Wisnom, Measurement and modelling of interlaminar shear strength enhancement under moderate through-thickness compression, Compos. Part A-Appl. S. 49 (2013) 18℮25.
[24] K.W. Gan, M.R. Wisnom, S.R. Hallett, Effect of high through-thickness compressive stress on fibre direction tensile strength of carbon/epoxy composite laminates, Compos. Sci. Technol. 90 (2014) 1℮8.
[25] P.J. Hine, R.A. Duckett, A.S. Kaddour, M.J. Hinton, G.M. Wells, The effect of hydrostatic pressure on the mechanical properties of glass fibre/epoxy unidirectional composites, Compos. Part A-Appl S. 36 (2) (2005) 279℮289.